

## N-doped titania-based nanofiber thin films synthesized via a hydrothermal route and their photo-induced properties under visible light

M. Grandcolas<sup>a,\*</sup> and J. Ye<sup>b</sup>

<sup>a</sup>International Center for Young Scientists (ICYS), National Institute for Materials Science (NIMS), 1-2-1 Sengen, Tsukuba, Ibaraki 305-0047, Japan

<sup>b</sup>Photo-Catalytic Materials Center (PCMC), National Institute for Materials Science (NIMS), 1-2-1 Sengen, Tsukuba, Ibaraki 305-0047, Japan

Titania nanofibers were grown on a titanium substrate using a hydrothermal reaction in an aqueous, concentrated sodium hydroxide solution. Post annealing in an ammonia atmosphere produced N-doped one-dimensional structures with a titanium dioxide structure and visible light absorption. The samples were characterized by scanning electron microscopy (SEM), X-ray diffraction (XRD), UV-Vis, Raman and X-ray photoelectron spectroscopy (XPS). The as-synthesized films showed a red shift and strong visible light absorbance between 400 and 700 nm, which is attributed to a doping effect. Photocatalytic activity in the aqueous phase under visible light irradiation led to the complete degradation of methylene blue within the first 3 h of the reaction. A visible-light-driven superhydrophilic effect was also observed.

**Key words:** Nitrogen doping, Titanium dioxide, Photocatalysis, Visible light, Nanofibers, Hydrothermal reaction.

### Introduction

Titanium dioxide nanostructured materials have attracted considerable attention because they have numerous applications in fields such as solar cells [1], catalysis [2], biomedicine [3], ceramics [4] and photocatalysis [5]. In particular, one-dimensional TiO<sub>2</sub>-based materials have been extensively studied, as these novel materials possess a unique combination of physicochemical properties [6]. Among the various possible methods for preparing TiO<sub>2</sub>-based materials, a hydrothermal route allows the selective synthesis of nanotubes or nanorods in large amounts [7]. One-dimensional nanomaterials are of particular importance for light-harvesting systems because of the unique way by which they conduct electrons along one axis, the axis of the tube, which leads to less resistance and minimizes electrons loss.

Tian *et al.* were the first to demonstrate a one-step, templateless method for directly preparing large arrays of oriented titania one-dimensional nanomaterials as a continuous film [8]. They synthesized nanotubes up to 10 μm in length using the hydrothermal reaction of dip-coated TiO<sub>2</sub> particles on Ti foil in concentrated sodium hydroxide for 20 h. Miyauchi and Tokudome showed that this type of photocatalytic transparent thin films exhibits super-hydrophilicity under UV light [9], thus opening the door to various applications that take advantage of their

anti-fogging and self-cleaning properties. Other authors have demonstrated the growth of nanostructured titania films via hydrothermal reaction on different substrates using this same technique [10, 11, 12]. Sodium titanate nanotubes have also been grown directly on a titanium metal template using a hydrothermal reaction in concentrated sodium hydroxide without additional Ti sources [13]. Different sources of titanium can be used, such as Ti flakes [14], foil [15], NiTi alloy [16], or plates [17]. The production of photocatalytic anatase nanowire films by in situ oxidation of Ti plates has been reported recently [17]; the films exhibited photocatalytic degradation of phenol under UV light.

It is well known that the band gap of titania materials (i.e., 3.2 eV for TiO<sub>2</sub> anatase) permits the absorbance of only the UV component of solar light. In the search for efficient solar energy, much effort has been devoted to seeking photocatalysts with large absorption and high reactivity under visible light. It has been reported that TiO<sub>2</sub> photocatalysts doped with either anions (N [18], S [19], C [20], F [21], etc.) or cations (Pt [22], Fe [23], Cu [24], etc.) or co-doped with several ions (N-S [25], N-Fe [26]) have their absorption edge red-shifted to lower energies, which enhances the photocatalytic performance in the visible range. In particular, N-doped TiO<sub>2</sub> is known to be a promising visible-light photocatalyst, particularly as a thin film [27].

To the best of our knowledge, this is the first report of the synthesis, via a hydrothermal reaction of pure titanium, of N-doped one-dimensional titania-based nanostructures with photocatalytic activity under visible irradiation.

\*Corresponding author:  
Tel : +81-29-859-2646  
Fax: +81-29-859-2301  
E-mail: grandcolasm@gmail.com

## Experimental

### Preparation of substrates

Commercially pure titanium foil (0.1 mm, 99.99%, Nilaco Corp.) was cut into  $15 \times 15 \text{ mm}^2$  pieces. All specimens were cleaned ultrasonically in ethanol and acetone and dried under an  $\text{N}_2$  stream prior to any treatment.

### Hydrothermal synthesis and ammonia treatment

The clean Ti substrates were immersed in a 10 M NaOH solution with a filling fraction of 90% in a 100 ml Teflon autoclave, and then treated at  $130^\circ\text{C}$  for 6 h. Next, the substrates were rinsed with ethanol and dried at  $70^\circ\text{C}$ . They were then immersed in a 0.1 M HCl aqueous solution for 2 h and washed with distilled water until the pH of the rinsing solution reached 6.

Nitrogen doping was performed using a previously reported one-step doping procedure [28]. Titania-based thin films were annealed under an  $\text{NH}_3$  flow at  $400^\circ\text{C}$  for 4 h. After cooling the samples down to room temperature and flushing them with synthetic air, they were stored in a reduced-moisture atmosphere in complete darkness.

### Characterizations

The morphologies of the samples were observed by a field emission scanning electron microscope (FESEM, JEOL JSM7001F, accelerating voltage : 15 kV). The crystal structure was determined using an X-ray diffractometer (XRD, JEOL JDX-3500) operated at 40 kV and 30 mA using  $\text{Cu-K}\alpha$  radiation. The UV-visible diffuse reflectance spectra were examined at room temperature with a UV-visible (UV-Vis) spectrophotometer (UV-2500, Shimadzu Corp.). Raman spectra were measured using a laser Raman spectrophotometer (NRS-1000, Jasco) at room temperature. The power of the incident laser beam was 2 mW, and its monochromatic wavelength was 532 nm. The laser pulses were focused onto the surface of the sample with a spot size of approximately  $10 \mu\text{m}$  by using an optical microscope with a  $20\times$  objective lens. An X-ray photoelectron spectrometer (XPS, PHI Quantera SXM, ULVAC-PHI) using monochromatic  $\text{Al-K}\alpha$  irradiation (power, 100 W; beam diameter,  $100 \mu\text{m}$ ; incident angle,  $45^\circ$ ) was employed to determine valence states on the surface of powder samples.

### Photo-induced characterizations of the films

We tested the photocatalytic activity by observing the discoloration of a methylene blue (MB) solution under visible light irradiation. The MB degradation was performed with a 1 mM solution in a plastic beaker, with the film deposited in the solution and irradiated vertically with a visible lamp. All experiments were conducted at room temperature in air. The amount of MB decomposition, as indicated by the discoloration of the solution and the progressive disappearance of the peak at 664 nm, was determined by UV-visible spectrometry (UV-2500, Shimadzu, Japan).

The evaluation of photo-induced hydrophilicity on the

substrate was performed in air as follows: First, the films were stored in clean polypropylene boxes in the dark for about 1 week. After confirming the initial contact angles for water, the water droplets were blown with nitrogen gas, and the films were then irradiated in air with visible light ( $\lambda > 420 \text{ nm}$ ) emitted by a Xe lamp with a cut-off filter. The contact angles were measured by the sessile drop method with a contact angle meter (DM-300; Kyowa Interface Science Co, Japan), and the photoinduced hydrophilicity was determined from the changes in the contact angles for water as a function of irradiation time.

## Results and Discussion

### Material characterizations

We used SEM imaging to investigate the morphology of the sample surfaces. Fig. 1 shows SEM images of a Ti foil before and after the hydrothermal treatment. Before treatment, the Ti foil had a smooth surface with typical machined channels and edges. After the hydrothermal treatment the morphology of the surface layer was slightly different from that of pure titanium, with the major difference being the existence of a myriad of one-dimensional nanostructures, from a few nanometres in diameter to several thousands in length and an average thickness of 200 nm, which made the surface much rougher. This nanofiber thin layer, which was produced by the hydrothermal reaction and was presumably composed of titanium dioxide, covered the surface of the substrate evenly. No morphological changes were observed when comparing the surface before and after the treatment under ammonia at  $400^\circ\text{C}$ .

Light absorption characteristics of the titania nanofibers was clearly affected by the modification of the thin film by the ammonia treatment. A simple visual observation

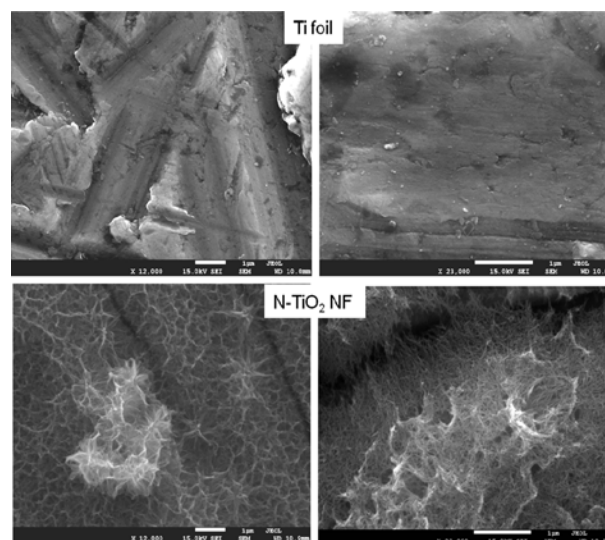


**Fig. 1.** SEM images of a titanium foil surface (Ti foil) before (top) and after (bottom) the hydrothermal reaction and ammonia treatment ( $\text{N-TiO}_2$  NF).

clearly showed a change in the color of the sample. After the hydrothermal reaction, a light photochromism was observed on the surface, produced by the growth of nanofibers. After the ammonia treatment, the sample turned yellowish gold. Furthermore, the UV-Vis spectra in Fig. 2 show a significant difference in absorption at wavelengths below 380 nm after the hydrothermal treatment. We attribute the intense band at these absorption wavelengths to the intrinsic band gap absorption of titanium oxide. From the transformed Kubelk-Munk function, the band gap ( $E_g$ ) can be determined to be 3.2 eV, which is in good agreement with the reported value for anatase (3.2-3.3 eV). After the doping process, we also observed a slight red shift in the peak around 380 nm as well as a large absorption band between 400 and 700 nm, indicating that the presence of N in the sample definitely improves the visible light absorption. This increase in the absorption spectra at wavelengths higher than 400 nm can be attributed to intrinsic doping levels.

Raman spectroscopy usually offers more information

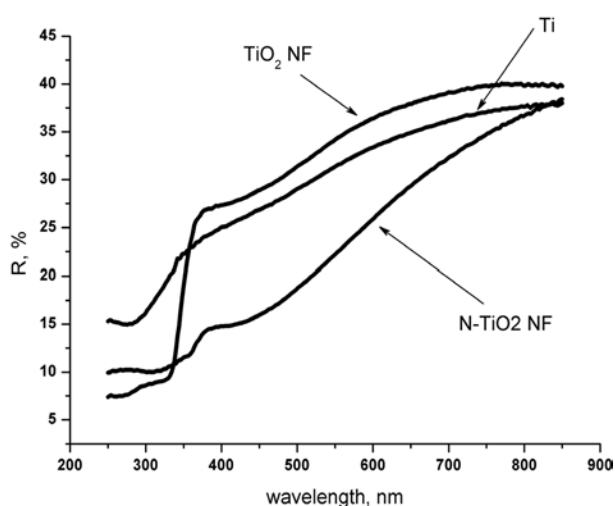


**Fig. 2.** UV-Vis spectra of pure titanium (Ti),  $\text{TiO}_2$  nanofibers ( $\text{TiO}_2$  NF) and N-doped  $\text{TiO}_2$  nanofibers (N- $\text{TiO}_2$  NF).

concerning the surface region compared to XRD, which mainly provides information about the bulk material, so we used the Raman method to characterize the sample more precisely. Fig. 3(a) shows a Raman spectroscopy pattern of the film after treatment, and strong bands at 145, 197, 397, 516, and 640  $\text{cm}^{-1}$  can be observed. All of these bands can be assigned to the anatase phase, and in particular, they can be assigned to the five Raman-active modes of anatase phase with the symmetries of Eg, Eg, B1g, A1g, and Eg, respectively [29].

We analyzed the crystal structures of the synthesized specimens with XRD. Fig. 3(b) shows the XRD patterns of the film as well as the substrate. A weak peak at  $25^\circ$  confirms the formation of the anatase phase. Taking into account the penetration depth of the X-ray beam, we attribute the major peaks on the spectrum to the titanium substrate.

We conducted X-ray photoelectron spectroscopy to investigate the chemical bonding state of the elements under investigation. Table 1 gives the XPS data for the atomic percentages of Ti, O, N, and C atoms in the sample. The atomic ratio between titanium and oxygen was about 0.48, which is in good agreement with the assumed chemical structure of  $\text{TiO}_2$ . The N doping level of this sample as estimated from the XPS spectra was about 1.4 at.%.

Fig. 4(a) shows the Ti 2p XPS spectrum, indicating the spin-orbit split lines of Ti 2p<sub>3/2</sub> and Ti 2p<sub>1/2</sub> to be at 458.7 and 464.6 eV, respectively, which is characteristic of the Ti (IV) oxidation state. No reduced signal of Ti (III) was observed. However, the peak of Ti 2p<sub>3/2</sub> shows a slight shift toward a lower band energy compared with

**Table 1.** Atomic percentage of elements detected by XPS analysis

Elements	Atomic % N-dopednanofibers
O1s	54.6
Ti2p	26.2
C1s	17.3
N1s	14

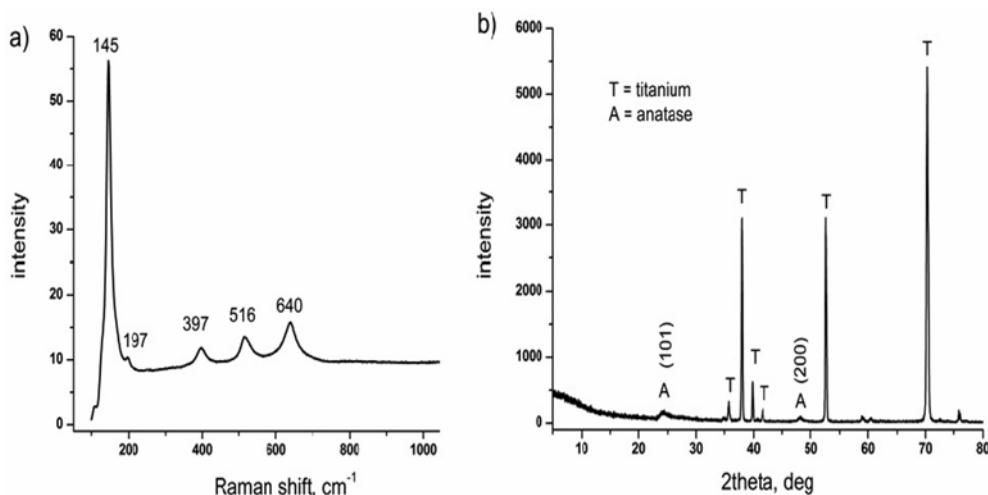


**Fig. 3.** (a) Raman spectrum, (b) XRD patterns of N-doped  $\text{TiO}_2$  nanofibers thin film.

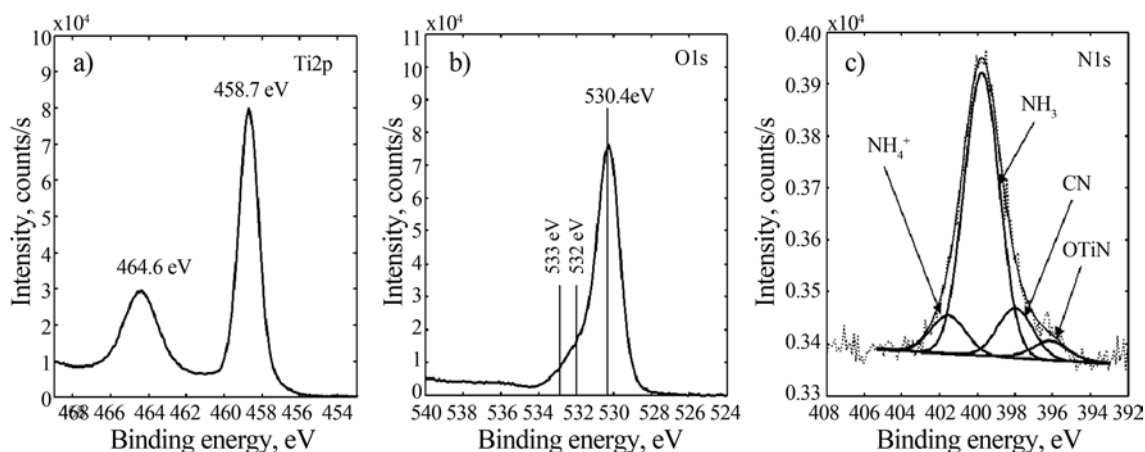


Fig. 4. N-doped TiO<sub>2</sub> nanofibers room temperature XPS spectra lines of (a) Ti 2p, (b) O 1s and (c) N 1s.

what the literature reports for pure crystalline TiO<sub>2</sub> [30]; the shift may be caused by the nitrogen doping. Fig. 4(b) shows the O 1s XPS spectrum, which exhibits a strong major peak at 530.4 eV, which is characteristic of the oxides of transition metals. Peaks at 532 and 533 eV can be attributed to hydroxyl groups on the surface of the photocatalyst and contamination with carbon compounds. Fig. 4(c) shows the N 1s XPS spectrum, which has a clear asymmetric broad peak centered at around 400 eV, indicating that more than one chemical state of nitrogen exists in the sample. By fitting the experimental spectrum profile, we identified four different peaks at 401.6, 399.8, 398.2, and 396.1 eV. The attribution of these peaks to specific compounds or chemical bonds has recently been the subject of vigorous debate and differs with the synthetic method used in each case. The peak at 396.1 eV is assigned here to anionic N-doping O-Ti-N, where oxygen atoms are replaced by nitrogen atoms involving substitutional N-doping [31]. The peak at 398.2 eV is due to contamination with carbon compounds. The peaks at 399.8 and 401.6 eV are attributed to some molecular nitrogen compounds adsorbed on the surface of TiO<sub>2</sub>, such as NH<sub>x</sub> and NO<sub>x</sub>.

### Photocatalytic activity

We performed visible light (> 420 nm) driven photocatalytic degradation of methylene blue over the N-doped TiO<sub>2</sub> nanofibers thin film, and results are presented in Fig. 5(a). For comparison, an undoped titania nanofiber film was used as the reference sample. We also performed MB photolysis under visible light irradiation, and it showed a progressive removal of the dye up to a maximum of 20% after 3 h of irradiation. The decrease in absorbance of the MB solution over undoped titania nanofibers was similar to that produced by the photolysis process, indicating that this sample was inactive for MB degradation under visible light irradiation. In contrast, the N-doped nanofiber thin film showed a high degradation rate for MB under visible light. The photocatalytic activity of the N-doped TiO<sub>2</sub> nanofibers was nearly three times greater than that of the undoped material, with a complete disappearance

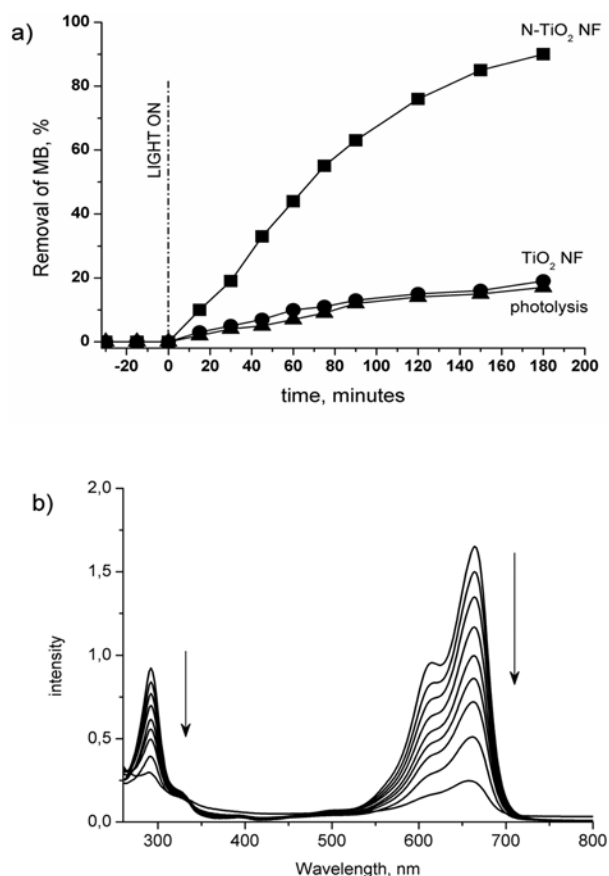


Fig. 5. (a) Percentage of removal of methylene blue in the presence of TiO<sub>2</sub> nanofiber (TiO<sub>2</sub> NF) and N-doped TiO<sub>2</sub> nanofiber (N-TiO<sub>2</sub> NF) thin films, and photolysis under visible light irradiation, (b) UV-Vis spectra vs time under visible light irradiation showing degradation of aromatic rings of MB in the presence of N-TiO<sub>2</sub> NF.

of MB within 3 h. The solution also changed color from deep blue to colorless. This enhanced photocatalytic ability can be ascribed to the N doping. When an electro-negative atom such as nitrogen is incorporated into the TiO<sub>2</sub> lattice, the dopant level appears between the valence band and the conduction band of titania, thereby altering the bandgap energy and shifting the absorbance edge to the visible

light region. Upon illumination with visible light, N-doped TiO<sub>2</sub> nanofibers generate electron-hole pairs at the tail states of the conduction and valence bands. The electrons generated in this way transfer to the adsorbed MB molecule on the particle surface because it is a cationic dye. This can increase the surface trapping rate of the carrier and retard the electron-hole recombination. Thus, an excited electron from the photocatalyst conduction band enters into the molecular structure of MB and disrupts its conjugated system, which leads to the complete decomposition of MB [32].

We can also observe in Fig. 5(b) the absorbance spectra of MB solution before and during the photocatalytic reaction. The peaks between 600 and 700 nm can be assigned to the absorption of the conjugated  $\pi$ -system, while the peaks close to 300 nm are assigned to the absorption of aromatic rings [33]. We were able to observe the progressive disappearance of all original peaks during the irradiation period; no new peak could be observed after 3 h of reaction, indicating that all aromatic rings disappeared and that the MB degraded completely [34].

### Water contact angle

We determined the photoinduced hydrophilicity from the changes in the contact angles for water under visible light irradiation (Fig. 6). The average contact angles for water on as-received titanium foil and on the foil after ultrasonic cleaning in a mixture of acetone and ethanol were 82.8° and 70.5°, respectively. The improvement in surface wettability was due to the removal of various organic species from the as-received specimen, and it illustrates the difference that can exist between real samples and the chemically-cleaned samples used in laboratory experiments. The initial contact angles after hydrothermal treatment and after the doping process were significantly lower, with both cases having an average angle of roughly 20°. The decrease can be explained by the chemical structure

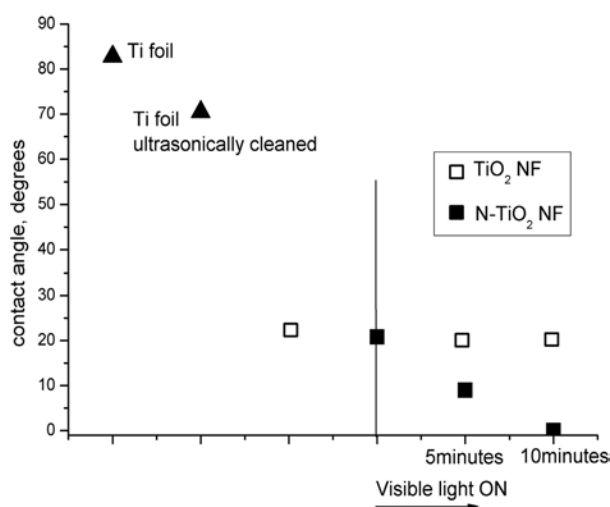


**Fig. 6.** Change in the water contact angle on different samples : Ti foil (▲), TiO<sub>2</sub> nanofiber thin film (□), and N-doped TiO<sub>2</sub> nanofiber thin film (■).

modification that takes place going from pure titanium to the titania TiO<sub>2</sub> phase. Irradiating with visible light (420 nm) caused the contact angle to decrease, and the film became superhydrophilic in 10 minutes. In comparison, a similar experiment was conducted on titania nanofibers without doping, and no effective decrease in the contact angle was observed.

### Conclusions

We successfully prepared nitrogen-doped TiO<sub>2</sub> nanofiber thin films by a simple two-step synthesis, specifically a hydrothermal reaction in a concentrated NaOH solution and post-annealing in ammonia vapor at 400 °C. The resulting N-doped thin film was observed to decompose methylene blue and to become superhydrophilic under visible light irradiation. The doped thin film was found to have a greater ability to decompose MB than an unmodified TiO<sub>2</sub> film in the present conditions. Further research is being conducted on using other modifications to enhance the harvesting of visible light.

### Acknowledgments

This work was supported by the International Center for Young Scientists (ICYS) of the National Institute for Materials Science (NIMS), Tsukuba, Japan. The author is grateful to Dr H. Iwai (Materials Analysis Station, NIMS) for XPS analysis and H. Gao for valuable help on SEM.

### References

1. B. O'Regan and M. Gratzel, *Nature* 353 (1991) 737.
2. B.M. Reddy, I. Ganesh and A. Khan, *J. Mol. Catal. A* 223 (2004) 294.
3. M. Navarro, M.P. Ginebra, J. Clément, S. Martinez, G. Avila and J.A. Planell, *J. Am Ceram. Soc.* 86 (2003) 1345.
4. S. Tursiloadi, H. Imai, H. Hirashima and J. Non-Cryst. Solids 350 (2004) 271.
5. M. Grandcolas, M. Karkmaz-Le Du, F. Bosc, A. Louvet, N. Keller and V. Keller, *Catal. Lett.* 123 (2008) 65.
6. H.H. Ou and S.L. Lo, *Separation Purif. Technol.* 58 (2007) 179-191.
7. T. Kasuga, M. Hiramatsu, A. Hoson, T. Sekino and K. Niihara, *Langmuir* 14 (1998) 3160-3163.
8. Z.R. Tian, J.A. Voigt, J. Liu, B. McKenzie and H. Xu, *J. Am. Chem. Soc.* 125 (2003) 12384-12385.
9. M. Miyauchi and H. Tokudome, *J. Mater. Chem.* 17 (2007) 2095-2100.
10. V.G. Pol and A. Zaban, *J. Phys. Chem. C* 111 (2007) 14574-14578.
11. Y. Guo, N.H. Lee, H.J. Oh, C.R. Yoon, K.S. Park, W.H. Lee, Y. Li, H.G. Lee, K.S. Lee and S.J. Kim, *Thin Solid Films* 516 (2008) 8363-8371.
12. Y. Su, N. Ma, X. Quan and H. Zhao, *Separ. Purif. Technol.* 68 (2009) 255-260.
13. M. Yada, Y. Inoue, M. Uota, T. Torikai, T. Watari, I. Noda and T. Hotokebuchi, *Langmuir* 23 (2007) 2815-2823.
14. Y. Guo, N.H. Lee, Y.J. Ho, C.R. Yoon, K.S. Park, H.G. Lee, K.S. Lee and S.J. Kim, *Nanotechnology* 18 (2007) 295608.

15. M. Kitano, R. Mitsui, D.R. Eddy, Z.M.A. El-Bahy, M. Matsuoka, M. Ueshima and M. Anpo, *Catal. Lett.* 119 (2007) 217-221.
16. S. Wu, X. Liu, T. Hu, P.K. Chu, J.P.Y. Ho, Y.L. Chan, K.W.K. Yeung, C.L. Chu, T.F. Hung, K.F. Huo, C.Y. Chung, W.W. Lu, K.M.C. Cheung and K.D.K. Luk, *Nanolett.* 8 (2008) 3803-3808.
17. Y. Wu, M. Long, W. Cai, S. Dai, C. Chen and D. Wu, J. Bai, *Nanotechnology* 20 (2009) 185703.
18. R. Asahi, T. Morikawa, T. Ohwaki, K. Aoki and Y. Taga, *Science* 293 (2001) 269-271.
19. T. Umebayashi, T. Yamaki, H. Ito and K. Asai, *Appl. Phys. Lett.* 81 (2002) 454-456.
20. S.U.M. Khan, M. Al-Shahry and W.B. Ingler, *Science* 297 (2002) 2243-2245.
21. A. Hattori, K. Shimoda, H. Tada and S. Ito, *Langmuir* 15 (1999) 5422-5425.
22. M. Anpo, K. Chiba, M. Tomonari, S. Coluccia, M. Che and M.A. Fox, *Bull. Chem. Soc. Jpn.* 64 (1991) 543-551.
23. G.N. Schrauzer and T.D. Guth, *J. Am. Chem. Soc.* 99 (1977) 7189-7193.
24. G. Colon, M. Maicu, M.C. Hidalgo and J.A. Navio, *Appl. Catal. B* 67 (2002) 41-51.
25. J. Yu, M. Zhou, B. Cheng and X. Zhao, *J. Mol. Catal. A* 246 (2006) 176-184.
26. X. Li, Z. Chen, Y. Shen and Y. Liu, *Powder Technol.* 207 (2011) 165-169.
27. M. Kitano, K. Funatsu, M. Matsuoka, M. Ueshima and M. Anpo, *J. Phys. Chem. B* 110 (2006) 25266-25272.
28. H. Irie, Y. Watanabe and K. Hashimoto, *J. Phys. Chem. B* 107 (2003) 5483-5486.
29. T. Ohsaka, F. Izumi and Y. Fijiki, *J. Raman Spectroscop.* 7 (1978) 321-324.
30. N.C. Saha and H.G. Thompkins, *J. Appl. Phys.* 72 (1992) 3072-3079.
31. J.F. Rengifo-Herrera, E. Mielczarski, J. Mielczarski, N.C. Castillo, J. Kiwi and C. Pulgarin, *Appl. Catal. B* 84 (2008) 448-456.
32. Y. Yang, H. Wang, X. Li and C. Wang, *Mater. Lett.* 63 (2009) 331-333.
33. P. Qu, J. Zhao, T. Shen and H. Hidaka, *J. Mol. Catal. A* 129 (1998) 257-268.
34. J. Tang, Z. Zou, J. Yin and J. Ye, *Chem. Phys. Lett.* 382 (2003) 175-179.